JOURNAL OF NANO- AND ELECTRONIC PHYSICS
Vol. 8 No 4, 04070(4pp) (2016)

ЖУРНАЛ НАНО- ТА ЕЛЕКТРОННОЇ ФІЗИКИ
Том 8 № 4, 04070(4cc) (2016)

The Dielectric Function of Metal 1D-systems

A.V. Korotun*, V.P. Kurbatsky, V.V. Pogosov

Zaporizhzhya National Technical University, 64, Gogol St., 69063 Zaporizhzhya, Ukraine

(Received 26 August 2016; revised manuscript received 19 December 2016; published online 23 December 2016)

The dielectric tensor diagonal components for metal nanowires of different metals have been calculated within the model of free electrons and a cylindrical potential well. The smooth size dependence of the Fermi energy has been compared with the results of the numerical calculations. The influence of the system dimensionality on the frequency dependence of the dielectric tensor has been investigated.

Keywords: Nanowire, Dielectric tensor, Fermi Energy, Oscillations, Frequency dependence.

DOI: 10.21272/jnep.8(4(2)).04070 PACS numbers: 73.21.Hb, 79.67.Lt

1. INTRODUCTION

Currently, much attention is devoted to the investigation of metal nanowires in connection with broad perspectives of their application in nanoelectronics [1-3]. In particular, metal 1D systems are used as optical antennas [4-6] in spectroscopy to increase the Raman scattering cross-section [7] and as dedicated probes for near-field microscopy [8].

A characteristic feature of these systems is the anisotropy of their optical properties due to the size quantization effects. In connection with this, such quantities as the optical conductivity or the dielectric function acquire a tensor character [9, 10].

The purpose of this paper is to calculate the dielectric tensor diagonal components of metal nanowires.

2. BASIC RELATIONS

As a result of the anisotropy of the optical properties of reduced dimensional metal systems, the connection between the electric field induction $\mathbf{D}_\alpha$ and strength $\mathbf{E}_\beta$ components has a nonlocal nature [10]

$$\mathbf{D}_\alpha(\mathbf{r}, \omega) = \int \epsilon_{\alpha\beta}(\mathbf{r}, \mathbf{r}', \omega)\mathbf{E}_\beta(\mathbf{r}', \omega)d\mathbf{r}' . \quad (1)$$

To define the dielectric tensor $\epsilon_{\alpha\beta}$, we use the results of [11] generalized to the case of anisotropic systems

$$\epsilon_{\alpha\beta} = 1 - \frac{8\pi e^2\hbar^2}{m_e^2\Omega}\sum_{i,j}\frac{f_i - f_j}{\varepsilon_{ij} - \hbar\omega}\left\{\langle j|e^{-i\mathbf{qr}}\hat{p}_\alpha|i\rangle - \frac{1}{2}\hbar q_\alpha\langle j|e^{-i\mathbf{qr}}|i\rangle\right\}\left\{\langle i|e^{i\mathbf{qr}}\hat{p}_\beta|j\rangle + \frac{1}{2}\hbar q_\beta\langle i|e^{i\mathbf{qr}}|j\rangle\right\}. \quad (2)$$

Here, i is the imaginary unit ($i = \sqrt{-1}$); m_e is the free electron mass; Ω is the system volume;

$$f_i = \left\{\exp\left(\frac{\varepsilon_i - \varepsilon_F}{k_B T}\right) + 1\right\}^{-1}$$

is the filling factor of states with energy ε_i; $|i\rangle$ and $\langle j|$ are the vectors of the initial and final state, respectively, $\varepsilon_{ij} \equiv \varepsilon_i - \varepsilon_j$, T is the temperature. In what follows, we assume that $T = 0$.

In the case when an electromagnetic wave is incident perpendicular to the symmetry axis of the wire, in the zero approximation of the expansion of $\epsilon_{\alpha\beta}$ with respect to a small parameter $\rho_0/\lambda \ll 1$ (ρ_0 is the characteristic system size, λ is the wavelength), expression (2) takes the following form:

$$\epsilon_{\alpha\beta} = 1 - \frac{8\pi e^2\hbar^2}{m_e^2\Omega}\sum_{i,j}\frac{f_i - f_j}{\varepsilon_{ij}\left(\varepsilon_{ij}^2 - \hbar^2\omega^2\right)}\langle j|\hat{p}_\alpha|i\rangle\langle i|\hat{p}_\beta|j\rangle . \quad (3)$$

The absorption is taken into consideration by the replacement $\omega \to \omega + i/\tau$, and, as a result, for the dielectric tensor diagonal components we obtain

$$\epsilon_{\alpha\alpha} = 1 - \frac{8\pi e^2\hbar^2}{m_e^2\Omega}\sum_{i,j}\frac{f_i\left(\varepsilon_{ij}^2 - \hbar^2\omega^2 + \hbar^2/\tau^2 + i\,2\hbar^2\omega/\tau\right)}{\varepsilon_{ij}\left[\left(\varepsilon_{ij}^2 - \hbar^2\omega^2 + \hbar^2/\tau^2\right)^2 + 4\hbar^4\omega^2/\tau^2\right]}\left|\langle j|\hat{p}_\alpha|i\rangle\right|^2 , \quad (4)$$

where τ is the relaxation time.

To calculate the dielectric tensor diagonal components, we use the expressions for the matrix elements of the projections of the momentum operator obtained in [9]

$$\langle j|\hat{p}_\alpha|i\rangle = \begin{cases} \hbar k_{zp}\delta_{ij}, & \alpha = z; \\ -\frac{i\hbar}{2}\delta_{pp'}k_{mn}C_{mn}\mathbf{G}_{(-)}, & \alpha = x; \\ \frac{\hbar}{2}\delta_{pp'}k_{mn}C_{mn}\mathbf{G}_{(+)}, & \alpha = y, \end{cases} \quad (5)$$

where δ_{ij} is the Kronecker delta and

$$\mathbf{G}_{(\mp)} = \mathbf{J}_{(-)}\delta_{m-1,m'} \mp \mathbf{J}_{(+)}\delta_{m+1,m'} ;$$

$$\mathbf{J}_{(\mp)} \equiv C_{m\mp1,n}\int_0^{\rho_0} I_{m\mp1}\left(k_{m\mp1,n'}\rho\right) I_{m\mp1}\left(k_{mn}\rho\right)\rho d\rho ; \quad (6)$$

$$C_{mn} = \frac{\sqrt{2}}{\rho_0\left|I'_m\left(k_{mn}\rho_0\right)\right|} ;$$

$I_m(\xi)$ are the m-order Bessel functions; $n = 1, 2, \ldots$; the

* andko@zntu.edu.ua

prime denotes the derivative with respect to ξ; the numbers k_{mn} are the roots of the equation

$$J_m(k_{mn}\rho_0)=0. \quad (7)$$

Substituting formulas (6) and (7) into (4), after rather cumbersome transformations and separation of the real and imaginary parts of the dielectric function, we have

$$\mathrm{Re}\,\epsilon_{\alpha\alpha}=1-\frac{k_p^4}{k_\omega^4+\gamma^4}\left\{1+\frac{\gamma^2}{k_\omega^2}S(\omega,\rho_0)\right\}, \quad (8)$$

$$\mathrm{Im}\,\epsilon_{\alpha\alpha}=\frac{k_p^4\gamma^2}{k_\omega^2\left(k_\omega^4+\gamma^4\right)}\left\{1+S(\omega,\rho_0)\right\}, \quad (9)$$

where $\alpha=x,y$; $k_\omega^2=2m_e\omega/\hbar$; $\gamma^2\equiv 2m_e/\hbar\tau$;; $k_p^2=2m_e\omega_p/\hbar$; $\omega_p^2\equiv 4\pi\bar{n}e^2/m_e$ is the plasma frequency;

$$S(\omega,\rho_0)\equiv\frac{2}{Nm_e}\sum_{i,j}f_{mnp}k_{mn}^2C_{mn}^2\left\{\mathrm{F}_{(-)}+\mathrm{F}_{(+)}\right\}; \quad (10)$$

$$\mathrm{F}_{(\mp)}=\frac{\left(k_{mn}^2-k_{m\mp1,n'}^2\right)\left\{\left(k_{mn}^2-k_{m\mp1,n'}^2\right)^2-3k_\omega^4+\gamma^4\right\}}{\left[\left(k_{mn}^2-k_{m\mp1,n'}^2\right)^2-k_\omega^4+\gamma^4\right]^2+4k_\omega^4\gamma^4}\mathrm{J}_{(\mp)}^2; \quad (11)$$

f_{mnp} is the step function,

$$f_{mnp}=\begin{cases}1, & k_{mn}^2+k_{zp}^2<k_\mathrm{F}^2,\\ 0, & k_{mn}^2+k_{zp}^2>k_\mathrm{F}^2.\end{cases}$$

To carry out numerical calculations using formulas (8)-(11), they should be supplemented by a relation, which determines the Fermi level of the metal nanowire [9]

$$\bar{n}=\frac{2}{\pi^2\rho_0^2}\sum_{m,n}\sqrt{k_\mathrm{F}^2-k_{mn}^2}. \quad (12)$$

Here, summation occurs over all values of m and n, for which $k_{mn}<k_\mathrm{F}$.

3. RESULTS AND DISCUSSION

The calculations were conducted for the values of electron concentrations $\bar{n}=\left(4\pi r_s^3/3\right)^{-1}$; $r_s=3.01a_0$, $2.11a_0$ and $2.07a_0$ for Au, Cu and Al, respectively (a_0 is the Bohr radius; r_s is the average distance between electrons).

In Fig. 1 we present the size dependence of the Fermi energy of Au and Al wires. It has an "oscillating" form. However, in contrast to the size dependence of the Fermi energy of metal films [12], the change of ε_F in Fig. 1 has a chaotic form.

In the case of the film, the kinks in the size dependence (i.e. jumps of the derivative $d\varepsilon_\mathrm{F}/dl$, l is the film thickness) are regularly located with an approximately constant period $\Delta l\approx\pi/k_\mathrm{F}^0$. In the size dependence of the Fermi energy of the wire, the kink appears when the increasing radius ρ_0 reaches such a value $\rho_{0m'n'}$, at which the condition $k_{mn}<k_\mathrm{F}$ begins to be fulfilled for one more pair of numbers (m', n'), $a_{m'n'}=k_\mathrm{F}\rho_{0m'n'}$.

The distance between the neighboring kinks

$$\Delta d\approx\frac{2\left(a_{m'n'}-a_{mn}\right)}{k_\mathrm{F}^0}$$

is obtained by overlapping the roots of the different-order Bessel functions and varies, at first glance, randomly.

The oscillation amplitude in the wire and the film at $d\cong l$ are of the same order of magnitude. As in the case of the film, with increasing $d\to\infty$, the "period" Δd and the oscillation amplitude tend to zero.

The features of the size dependence of the Fermi energy of various metal nanowires are exclusively explained by different values of k_F^0. For Al wire, in comparison with Au wire, the oscillation scale Δd is smaller (since the root density $a_{mn}\approx k_\mathrm{F}^0\rho_0/\pi$ is larger), the amplitude and the smoothed value $\varepsilon_\mathrm{F}/\varepsilon_\mathrm{F}^0$ are smaller.

Let us use the results of numerical calculations shown in Fig. 1 to check the smoothed size dependence [8]

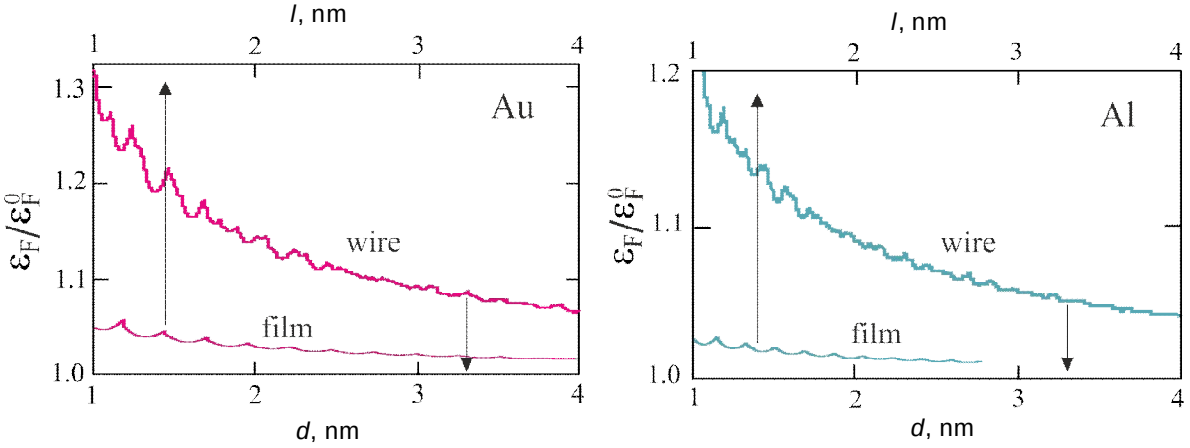

Fig. 1 – Size dependence of the Fermi energy of metal nanowires ($d=2\rho_0$) and films [10]

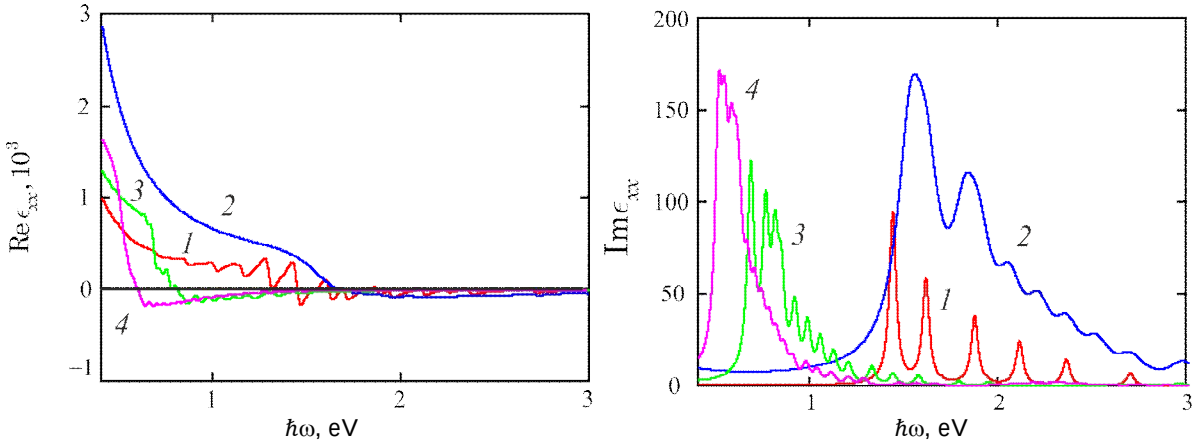

Fig. 2 – Frequency dependence of the dielectric tensor diagonal component of Au nanowires of different diameter

$$\frac{\varepsilon_F}{\varepsilon_F^0} = \frac{k_F^2}{k_F^{02}} \cong A^2 + \frac{2AB}{k_F^0 \rho_0}, \qquad (13)$$

where $A^2 = 1.10$, $AB = 1.22$.

$$\frac{\left(\frac{\varepsilon_F}{\varepsilon_F^0} - 1.10\right)_{Au}}{\left(\frac{\varepsilon_F}{\varepsilon_F^0} - 1.10\right)_{Al}} = \frac{\left(k_F^0\right)_{Au}}{\left(k_F^0\right)_{Al}} = \frac{1.75 \cdot 10^{10}}{1.21 \cdot 10^{10}} = 1.45 .$$

According to Fig. 1, for $d = 1$ nm

$$\frac{\left(\frac{\varepsilon_F}{\varepsilon_F^0} - 1\right)_{Au}}{\left(\frac{\varepsilon_F}{\varepsilon_F^0} - 1\right)_{Al}} \approx \frac{0.30}{0.19} = 1.58 .$$

If take into consideration a sufficiently large error in reading data Fig. 1, the agreement between the calculation results by formula (13) and the numerical calculation can be considered satisfactory.

Then we check the inverse relationship $\left(\frac{\varepsilon_F}{\varepsilon_F^0} - 1.1\right) \propto \frac{1}{d}$. The check results are given in Table 1 and show quite good agreement.

In Fig. 2 we illustrate the frequency dependences of the real and imaginary parts of the dielectric tensor diagonal component ϵ_{xx} of Au nanowires with a diameter of $d = 1.6$, 2, 3, 4 nm (curves 1-4, respectively). For Reϵ_{xx}, oscillations take place only for wires of 1.6 nm diameter and disappear with increasing diameter. The oscillation amplitude reaches the maximum value at $\hbar\omega \approx 1.5$ eV. While the values of Im$\epsilon_{xx}(\hbar\omega)$ shift to lower frequencies with increasing diameter, the oscillation amplitude increases, the distance between the peaks decreases, and the oscillations are smoothed for $d = 4$ nm. This is due to the fact that with increasing d, the number of levels of size quantization increases and, thus, the number of possible transitions between them.

Table 1 – $\left(\frac{\varepsilon_F}{\varepsilon_F^0} - 1.1\right) \propto \frac{1}{d}$ inverse relationship check results

No	d, nm	$\left(\frac{\varepsilon_F}{\varepsilon_F^0} - 1.1\right) \propto \frac{1}{d}$ by Fig. 1 for Au	$\left(\frac{\varepsilon_F}{\varepsilon_F^0} - 1.1\right) \propto \frac{1}{d}$ by formula (13)
1	1	1	1
2	1.5	0.64	0.67
3	2	0.47	0.50
4	3	0.31	0.33
5	4	0.23	0.25
6	5	0.18	0.20

In Fig. 3 we illustrate the frequency dependences of Imϵ_{xx} for various metal wires of $d = 4$ nm diameter. For Al, the dielectric function has one maximum and oscillations are absent. With increasing frequency, the oscillations are damped for both Cu and Au. Such a behavior of the dielectric function is explained by the small value of the relaxation time of Al electrons $\tau = 0.8 \cdot 10^{-14}$ s [13], so that the peak width is approximately $\hbar/\tau = 0.082$ eV compared with the other two metals.

Let us compare the calculation results of the dielectric function of metal nanowires with similar results for thin films [14]. The starting point, which can be formula (4) at $\alpha = x$, is the same for both cases (the film is oriented perpendicular to the x axis).

For a film of thickness l and longitudinal dimensions a and b ($l \ll a, b$), the expression for the dielectric function has the form of [14]

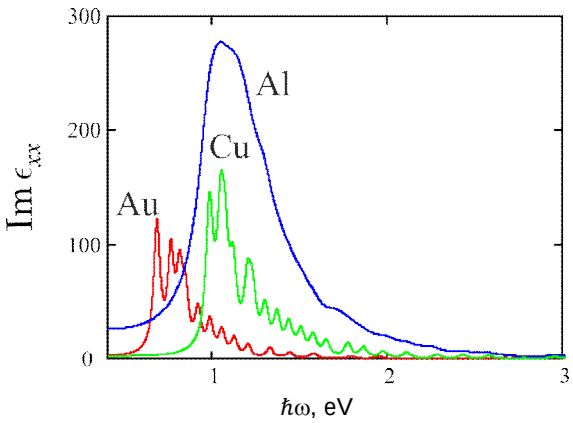

Fig. 3 – Frequency dependence of the imaginary part of the dielectric function for different metal wires

$$\mathrm{Re}\,\epsilon_{xx} = 1 + \left(\frac{4}{L}\right)^4 \frac{L}{a_0}\Phi_{(-)}, \qquad (14)$$

$$\mathrm{Im}\,\epsilon_{xx} = \left(\frac{4}{L}\right)^4 \frac{L}{a_0}\frac{\gamma^2}{k_\omega^2}\Phi_{(+)}, \qquad (15)$$

where

$$\Phi_{(\mp)} = \sum_{m=1}^{m_F}\sum_{m'=1}^{m_{\max}} \frac{k_{xm}^2 k_{xm'}^2 \left(k_F^2 - k_{xm}^2\right)\left\{1-(-1)^{m+m'}\right\}\left\{\left(k_{xm'}^2 - k_{xm}^2\right)^2 \mp k_\omega^4 \mp \gamma^4\right\}}{\left(1+2/L\kappa_m\right)\left(1+2/L\kappa_{m'}\right)\left(k_{xm}^2 - k_{xm'}^2\right)^3 \left\{\left(\left(k_{xm'}^2 - k_{xm}^2\right)^2 - k_\omega^4 + \gamma^4\right)^2 + 4\gamma^4 k_\omega^4\right\}}, \qquad (16)$$

$$m_F \equiv \left[\frac{Lk_F}{\pi} + \frac{2}{\pi}\arcsin\frac{k_F}{k_0}\right], \quad m_{\max} \equiv \left[\frac{Lk_0}{\pi}\right] + 1. \qquad (17)$$

The square brackets in (17) denote the integer part of the number. Since the calculation in [14] was performed for a well of finite depth U_0, then the quantities k_{xm} are the roots of equation

$$k_{xm}l = \pi m - 2\arcsin\left(\frac{k_{xm}}{k_0}\right), \qquad (18)$$

where $\hbar k_0 \equiv \sqrt{2m_e|U_0|}$; $\kappa_m \equiv \sqrt{k_0^2 - k_{xm}^2}$.

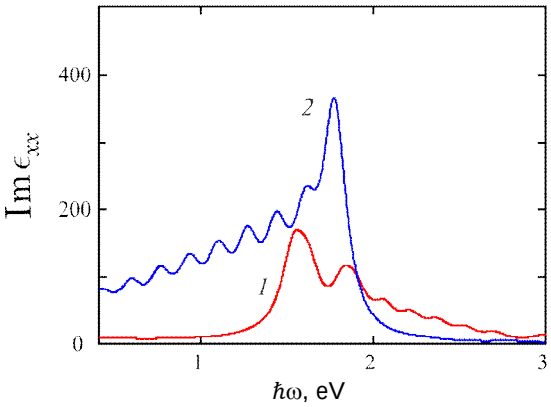

Fig. 4 – Frequency dependence of the imaginary part of the dielectric function of Al wire (1) and film (2)

In Fig. 4 we present the dependences $\mathrm{Im}\epsilon_{xx}(\hbar\omega)$ for Al wire of $d = 2$ nm diameter and Al film of $l = 2$ nm thick [14]. As seen from Fig. 4, oscillations occur in different frequency ranges: for the wire at $\hbar\omega > 1.8$ eV and for the film – at $\hbar\omega < 1.8$ eV. This is explained by the fact that the distances between the levels of size quantization are larger in the wire than in the film.

4. CONCLUSIONS

In this paper, the dielectric tensor diagonal components of metal nanowires have been calculated taking into account the size dependence of the Fermi energy. The comparison of the smoothed size dependence with the results of numerical calculations from the exact procedure has shown good agreement.

The evolution of the frequency dependences of the real and imaginary parts of the dielectric function through variation of the diameter has been studied. It has been established that with increasing wire diameter, the peaks shift to the left, the distance between them decreases and they overlap.

The behavior of the imaginary parts of the dielectric function for various metals is qualitatively similar, but is quantitatively different in that the values of $(\hbar\omega)_{\min}$, from which the oscillations begin, are different, because of the difference in the values of electron concentrations and relaxation times.

It has been shown that the frequency ranges, in which oscillations occur, are different for wires and films that is explained by the differences in the system dimensionality and the appearance of an additional restriction to the electron motion with decreasing system dimensionality.

REFERENCES

1. A. Gloskovskii, D.A. Valdaitsev, M. Nepijko, J. Lange, V. Aeschlimann, V. Bauer, M. Klimenkov, L.V. Viduta, P.M. Tomchuk, G. Schonhense, *Phys. Rev. B* 77 No 19, 195427 (2008).
2. A. Kumar, As. Kumar, P.K. Ahluwalia, *Phys. E* 46, 259 (2012).
3. K. Moors, B. Sorée, Z. Tokei, W. Magnus, arXiv:1503.08015v3.
4. A. Pucci, F. Neubrech, D. Weber, S. Hong, T. Toury, M. Lamy de la Chapelle, *phys. status solidi b* 247 No 8, 2071 (2010).
5. A.Ye. Krasnok, I.S. Maksimov, A.I. Denisyuk, P.A. Belov, A.Ye. Miroshnichenko, K.R. Simovskiy, Yu.S. Kivshar', *Usp.-Phys.* 183, 561 (2013).
6. D.A. Zuev, S.V. Makarov, I.S. Mukhin, S.V. Starikov, I.A. Morozov, I.I. Shishkin, A.E. Krasnok, P.A. Belov, *Adv. Mater.* 28 No 16, 3087 (2016).
7. M. Fan, G.F. Andrade, A.G. Brolo, *Anal. Chim. Acta* 693, 7 (2011).
8. T.H. Taminiau, F.D. Stefani, F.B. Segerink, N.F. van Hulst, *Nature Photon.* 2, 234. (2008).
9. V.P. Kurbatsky, A.V. Korotun, A.V. Babich, V.V. Pogosov, *Phys. Solid State* 51, 2371 (2009).
10. V.P. Kurbatsky, V.V. Pogosov, *Phys. Rev. B* 81, 155404 (2010).
11. D.M. Wood, N.W. Ashcroft, *Phys. Rev. B* 25, 6255 (1982).
12. V.P. Kurbatsky, V.V. Pogosov, *Phys. Solid State* 46, 543 (2004).
13. N. Ashkroft, N. Mermin, *Fizika tverdogo tela, T. 1* (Moskva: Mir: 1979).
14. V.P. Kurbatsky, A.V. Korotun, V.V. Pogosov, Ye.V. Vasyutin, *Phys. Solid State* 50, 949 (2008).